The Design

of

The PDX Tokamak Wall Armor and Inner Limiter System

H. W. Kugel and M. Ulrickson

Plasma Physics Laboratory, Princeton University

Princeton, New Jersey 08544

Abstract

The inner wall protective plates for the PDX Tokamak are designed to absorb 8 MW of neutral deuterium beam power at maximum power densities of 3 kW/cm^2 for pulse lengths of 0.5 sec. Preliminary studies indicate that the design could survive several pulses of 1 sec duration. The design consists of a tile and mounting plate structure. The mounting plates are water cooled to allow short duty cycles and beam calorimetry. The temperature and flow of the coolant is measured to obtain the injected power. A thermocouple array on the tiles provides beam position and power density profiles. Several material combinations for the tiles were subjected to thermal tests using both electron and neutral beams, and titanium carbide coated graphite was selected as the tile material. The heat transfer coefficient of the tile backing plate structure was measured to determine the maximum pulse rate allowable. The design of the armor system allows the structure to be used as a neutral beam power diagnostic and as an inner plasma limiter. The electrical and cooling systems external to the vacuum vessel are discussed.

1. Introduction

The Poloidal Divertor Experiment (PDX) is being used to study impurity control and other significant physical processes in high-temperature neutral beam heated plasmas. The PDX/ORNL neutral beam injection system [1-2] consists of 4 beamlines, and injects a total heating power of 6 MW H^o or 8 MW D^o. The injection is at a nearly perpendicular injection angle (9 degrees). The beamlines are positioned around PDX as shown in Fig. 1. The measured neutral beam power density profile in the focal plane is almost axially symmetric and approximately gaussian from the maximum power point to about 10% of maximum with a characteristic half-angle-at-1/e of 1.1° to 1.8°. A typical power density profile at the inner wall of PDX based on the Kim-Whealton model of beam divergence [3] is shown in Fig. 2 [4]. The expected maximum power density on beam axis at the inner wall of the torus for 300 msec injection is 3.2 kW/cm^2. Eventual 500 msec injection pulse lengths are anticipated. Incident power densities of this magnitude, for pulse durations of up to 500 msec, require the protection of the 0.95 cm thick 304 SS inner wall of PDX. The adopted armor plate consists of arrays of water cooled, titanium carbide coated graphite tiles, supported on the inner wall of the torus, opposite each beam port (Fig. 1). Titanium plates shield the gaps between the graphite units.

2. General Requirements

The PDX wall armor is designed to function as an inner wall thermal armor, a neutral beam power diagnostic, and a large area inner plasma limiter. The maximum PDX neutral beam power densities are capable of melting the surface of the 0.95 cm thick SS-304 inner wall in about 250 msec if injection occurs in the absence of a plasma, i.e., during conditions allowing essentially 100% power transmission to the inner wall. During normal operation with typical PDX plasma densities the beam transmission is ~ 10-30%, thus reducing the power density to the inner wall proportionately. However, if a disruption in the plasma current occurs during neutral beam injection, the transmitted power could increase to its maximum value. In principle, beam injection is terminated by a sense circuit ~ 10 msec after the disappearance of the plasma current. However, the PDX armor is designed to accommodate this range of conditions and increase the margin of safety by adequately shielding the inner wall of the torus from full power for 0.5 sec in the absence of a plasma.

In order to study neutral beam heating in PDX, it is desirable to measure injected power directly for a variety of beam and plasma conditions. The PDX inner wall armor has water cooling lines which are monitored for flow rate and temperature to give the total incident integrated power. The four separate water calorimeters can be used to calibrate the injected beam power for each beamline by performing the measurements in the absence of the plasma. In addition, the integrated beam power transmitted through the plasma to the calorimeters can be measured for each plasma shot. This information is useful for interpreting neutral beam heating results and for optimizing the total injected power.

Each calorimeter unit has an array of 14 to 16 thermocouples implanted close to the front surface of the graphite. The thermocouple signals are transmitted via a CAMAC data highway to a DEC PDP 11/34 computer to give displays of beam position and beam power density profiles at the inner wall.

Window ports on the outer wall of the torus permit the use of pyrometers and IR cameras to give the front face temperature of the armor at the regions of maximum power deposition. Such measurements provide a safety diagnostic for monitoring the integrity of the armor and also yield useful information on armor front face temperature profiles and effective heat transfer coefficients.

The PDX inner wall armor is designed to also function as a plasma limiter. It has been estimated that a conventional poloidal rail inner limiter has a peak plasma thermal load of the order of 2 kW/cm^2 at mid-plane, whereas for an axisymmetric toroidal limiter, the peak plasma thermal load at mid-plane would be about 200 W/cm^2 [5]. This substantially lower thermal load for a toroidal limiter is expected to provide a reduction in limiter impurity emissions, and thermal fatigue. The PDX toroidal limiter configuration will contribute useful information concerning plasma and disruption thermal loads for a nearly axisymmetric limiter, impurity emissions, surface damage, mechanical stability, and overall reliability.

3. Material Criteria

The following material criteria were established to allow the selection of candidate armor materials that meet the various constraints imposed by the PDX environment. It is desirable that the candidate material for the front face of the armor be able to accept full power injection for 0.5 sec at a maximum power density of 3 kW/cm^2. In addition, for future contingency, the armor should be able to accept an ~ 10% upgrade in neutral beam power. The PDX duty cycle is typically 1 pulse every 300 sec. It is desirable to have an armor cool-down time of ~ 180 sec. This will prevent thermal racheting during an experimental run. The experimental schedule for PDX will require ~ 10^4 pulses per year. The armor front face material should withstand ~ 10^3 unattenuated beam strikes of 0.5 sec duration and ~ 10^4 beam strikes at ~ 20% of full power for each year of its planned five year life. In addition the armor material should have sufficient mechanical strength to endure disruption induced eddy current forces over its entire operating temperature regime.

Plasma impurities provide thermal loss mechanisms, affect stability, control, and deleterious impurity effects increase with the atomic number (Z) of the impurity [6-7]. Hence, it is desirable that the candidate materials have as low a Z as possible given the other constraints. In addition the armor material should have low physical and chemical sputtering yields over its operating regime. The candidate armor material should not act as a reservoir of H and/or D, since this will complicate plasma control and quick operating isotope changes desired for experimental purposes. The material chosen should have outgassing rates consistent with PDX vacuum requirements.

The inner wall of PDX supports magnetic field sensing elements, microwave horns, and various mirrors and opaque field-of-view-stops ("dumps") for microwave, IR, optical, UV, and X-ray diagnostics. It is desirable that the armor material and its configuration provide the minimum possible perturbation to these diagnostics. Several candidate materials seemed promising in terms of their physical properties, but availability or ease of fabrication presented formidable difficulties.

4.0 Materials Issues

Table 1 shows typical sputtering coefficients for the candidate materials. It is seen that Ti and V have lower sputtering yields than Cu. The sputtering yield for TiC is much lower than that of graphite. Table 1 also lists the melting points and sublimation temperatures. It is seen that armor with Ti or V cladding would have a substantially higher front face melting point than unclad Cu.

The long term impurity outgassing from samples of thin titanium explosively bonded to 1.3 cm OFHC copper (Ti/Cu) and thin vandium explosively bond to 1.3 cm OFHC copper (V/Cu) has been found comparable to that of the bulk substrate [8]. Measurements of the outgassing from an unbaked sample of POCO graphite [9] coated with a 15 μm thick layer of vapor deposited titanium carbide [10] (TiC/C) have been performed up to 800°C using a residual gas analyzer. The results indicate the presence of predominantly hydrogen with amounts of typical hydrocarbons at levels acceptable to the PDX environment [11]. Recent work [12] has shown that initial CD_4 production in TiC/C from implanted deuterium reaches a peak (0.02–0.03 CD_4/incident D) at a substrate temperature of 100–200°C and decreases by an order of magnitude at 350°C. After a high initial rate, methane production was found to decrease slowly to values substantially lower than the peak rate. The high initial rates could be recovered by annealing the samples at 1000°C for 30 minutes. This behavior is similar to that found for SiC in previous work [13] where the decrease in methane production was attributed to the formation of an outer layer in the SiC which was depleted in carbon. Sufficient annealing at high temperatures restores the initial methane production by allowing bulk carbon to diffuse into the depleted region. Similar measurements of methane production in graphite exhibit a uniform production rate with bombardment time and find a maximum value of ~ 0.06–0.08 CD_4/incident D at 500°C [14]. Hence, it appears that the use of relatively large amounts of TiC/C in a tokamak/neutral beam environment may benefit from an initial conditioning period to reduce methane production followed by sufficient temperature controls to minimize annealing at high temperatures.

Previous material studies [15] have shown that both TiC/C and V/Cu have thermal shock and thermal fatigue thermal flux limits which are adequate for the PDX requirements. Of these two material combinations the TiC/C system is the more developed and has not exhibited any failures under anticipated PDX conditions in the testing done to date. It thus appears to be the most reliable material choice from a thermal standpoint.

The V/Cu material armor is more convenient to machine than TiC/C and could be fabricated in larger sections. It would also be more durable during installation and subsequent maintenance due to the much greater thickness of its cladding. However, the explosive bonding process at present can only be used to cover large flat surfaces, and, hence, it leaves unclad edges and corners. Vanadium cladding on the edges and corners can be achieved by rolling the edges of large Vi/Cu plates over a suitably small radius or by cutting and welding techniques. The application of these methods to the edge problem has not been explored extensively, and units fabricated in this manner have not been tested in cyclic high thermal fluxes.

In view of the constraints discussed above, and the PDX experimental schedule, the TiC/C system was selected as the optimum material for the PDX armor and inner limiter system.

5. Backing Plate and Support Constraints

The access to the PDX vessel is via 31 cm x 34 cm ports. This places a maximum size constraint on all armor components and installation procedures. The toroidal radius of curvature of the PDX inner wall is 71.4 cm. This relatively small radius of curvature requires armor segments of a comparable curvature or, equivalently, many narrow flat plates. However, practical constraints required the selection of a flat plate geometry of 9.93 cm front face width for the PDX armor design as a compromise between maximizing fl. . plate width in order to reduce the required total number of plates and minimizing the amount of plate-edge exposure and protrusion beyond the mean armor radius as the plate width is increased.

Figure 3 shows the position of the inner wall and armor relative to the separatrix and the last unshorted flux line. An armor front face distance of 13.3 cm between the wall and the armor was chosen as a compromise to accommodate inner wall diagnostics, armor cooling lines, and armor thermocouples (discussed below) and the front face distance from the separatrix. An armor length of 61 cm or 30.5 cm above and below the mid-plane was chosen to prevent protrusion beyond the shielding provided by the upper and lower inner limiters (see Fig. 3). The specification of this length determined the graphite tile dimensions. The 9.65 cm backing plate width was determined by the 9.93 cm tile width. The tile length was chosen so as to have an approximately square shape and an odd number of tiles per backing plate. An approximately square shape was desired to achieve a more symmetric thermal expansion. An odd number of tiles was chosen to eliminate any gap at the midplane where the neutral beam power is greatest.

The tile support mechanism was an important consideration in the design of the PDX armor system because it required compromises between several conflicting and severe constraints. It is of primary importance that the mount have sufficient mechanical strength to endure eddy current forces during disruptions in the plasma current, in addition to the strong vibrations that occur during normal operations. There must also be sufficient contact pressure to provide an adequate heat transfer coefficient between the tiles and the cooled backing plate to allow the desired duty cycle. However, these criteria conflict with the need to minimize cyclic thermal stress in the tiles under the assumed thermal loads. The design of the tile mount was chosen to give the smallest amount of thermal restraint consistent with the mechanical and heat transfer requirements.

It was found that these design criteria could be achieved by using a dove-tail attachment technique. Figure 4 shows a summary of the materials and designs tested for the back plates. The SS-304 backing plate has good mechanical strength over a wide temperature range, but it has poor thermal conductivity. The copper backing plate has good thermal conductivity but poor mechanical strength at elevated temperatures. The brazed hybrid combinations of copper and SS-304 with single and double dove-tails combine mechanical strength and good thermal conductivity. The tests of the candidate designs consisted of fabricating POCO graphite tiles to fit each of the dove-tail backing plate designs shown in Fig. 4. Each of these tile-backing plate combinations was heated uniformly to 500°C using an oxygen-acetylene torch. The heat source was then removed and 120 psi water was allowed to flow through the 0.48 cm I.D. cooling lines of the backing plate. The front face temperature change was measured as a function of time using an IR camera. The results are shown in Fig. 5. It is seen that the hybrid double dove-tail design (No. 4 in Fig. 4) had the fastest cool down and, hence, the highest heat transfer coefficient. This prototype was then subjected to 1000, 40 keV, 2.5 kW/cm^2, 250 msec neutral beam (H^o) shots and showed no evidence of deleterious effects. Figures 6a and 6b show the front face temperature of this prototype after one of the neutral beam shots of this test. The solid line is the theoretical thermal behavior expected using standard heat transfer theory [16]. An effective heat transfer coefficient of 0.05 watts/cm^2-C° was derived from these results and used to estimate a cooldown time of less than 180 sec, for a PDX full power, 500 msec neutral beam shot using water coolant at 120 psi. This prototype was adopted for the final design. Figures 7 and 8 show details of the final design for the tiles, backing plates, cooling lines, and support structure.

The dove-tail design together with a 0.076 cm expansion gap and molybdenum flat springs allow the free expansion and bending of the tile into the dove-tail gap minimizing thermal stresses while maintaining strong mechanical support. The expansion gap and dove-tail dimensions were chosen so that the residual cyclic thermal stress in the corners of the dove tails are within the stress capabilities of graphite. The molybdenum springs maintain the expansion gap and good thermal contact at the dove tails.

Each armor backing plate has four 0.48 cm I.D. copper cooling lines which are vacuum brazed between its SS-304 and copper sections. The four cooling lines were fabricated from a continuous tube and positioned as close as possible to the edge of the dove-tails (see Fig. 7). A thermal expansion gap of 0.229 cm is provided between the graphite backing plates at the front face of the tiles to accommodate a brief tile front face temperature of as high as 3000°C. The tile thickness and the angle of incidence of the beam combine to adequately shield the inner wall region that is directly behind these expansion gaps.

The lower part of the backing plates are bolted firmly to curved rails which are attached to the inner wall (see Fig. 8). The upper part of the backing plates are held and guided by bolts which are configured to allow a 0.64 cm vertical thermal expansion of the backing plates before being restrained by the bolt heads.

6. Cooling System

It is desirable that the coolant provide a heat transfer coefficient in the range of 0.6 to 6 watts/cm^2-°C for full power, 0.5 sec pulse lengths. Several cooling system alternatives were investigated. The primary issues in the consideration of various coolants involved the consequences of a cooling line failure in the vacuum environment of PDX. If a leak should occur in the interior of the PDX vacuum vessel, the coolant properties should allow a rapid recovery to acceptable vacuum and plasma conditions. In particular, given the probability of an internal cooling line failure during either hot or cold surface conditions, the coolant should be of low Z, of low chemical reactivity, relatively volatile, and easily removable by pumping and glow discharge cleaning. The cooling system, for experimental convenience, should not require a very low temperature coolant or a very high temperature coolant. In addition, the cooling system should have long term operational reliablility and a stable, known heat transfer efficiency.

Several cooling system alternatives for PDX were investigated. High pressure helium gas cooling, a primary liquid coolant loop containing one of several candidate coolants, and a segmented system with fast isolation values and water coolant were considered. The results indicate that each method is technically feasible.

Helium gas cooling would do the least harm to the PDX vacuum environment in the event of a cooling line failure. However, helium gas cooling appears to be the least cost effective for PDX since it is the most expensive and gives a much smaller heat transfer coefficient for acceptable system sizes. In addition, it would require the longest lead time to implement, and it would be the least reliable in terms of maintenance and stability.

A closed primary liquid cooling loop was considered for all four armor units or for each of four armor units containing a net volume of liquid coolant available for leakage of 1 to 2 liters, depending on the geometry and interlocks methods. A large number of refrigerants, reactor coolants, and liquid hydrocarbons were compared with the design criteria. The acceptable candidates were H_2O and certain liquid hydrocarbons of the form C_xH_y containing no oxygen bonds and having boiling points greater than 100 C.

The cooling method finally adopted for the PDX armor consists of a separate water cooled system for each of the armor units. The results of our analysis indicated that this cooling method for the PDX armor has the advantage of being simple, reliable, easily maintained, stable, efficient and non-toxic. The disadvantages of water pertain to its oxidizing ability and vapor pressure, and these properties were considered in the cooling system design. The system was designed with interlocks (discussed below) which limit the possible water leakage into the vacuum vessel in the event of a cooling line failure to less than 2 liters per armor unit. It is believed that this amount of liquid would collect in the lowest protruding ports of the vacuum vessel and could be easily removed. The residual water could be removed by vacuum pumping and glow discharge cleaning [17]. It is estimated that about 1 week of glow discharge cleaning would be required to achieve an acceptable vacuum in PDX after such an occurrence [18].

Each of the four armor units consists of three subunits containing either two or three backing plates. The copper cooling lines from the individual backing plates were brazed to 1.91 cm O. D., SS-304 water supply and drain manifolds. The manifolds from each subunit were joined with Conflat flanges and copper gaskets (Fig. 9). All brazing and welding of this part of the manifold system was performed outside of PDX in order to achieve the highest possible reliability and to help preserve the ultra clean vacuum environment of PDX. The supply and drain manifolds are connected to shielded flexible stainless steel hoses. The flexible hose is certified for 2000 psi service, and thus is adequate for use in the PDX vacuum with a 120 psi water system. Rubber hose is used outside of the vacuum vessel to maintain its electrical isolation.

Fast, air actuated, solenoid values are interlocked to the main PDX vacuum pressure gauge. An unacceptable PDX vacuum pressure will inhibit neutral beam injection, close the fast solenoid values, and stop the water flow. Manual valves on each of the four armor water systems allow the residual water in the line to be immediately ejected by high pressure He gas and then evacuated by a mechanical vacuum pump. Each armor water system is equipped with a turbine flow meter and a thermocouple for measuring water flow and temperature. Although the primary purpose of these instruments is to obtain a measure of the total power incident on the armor, they are also monitored by control circuits to assure water flow and cooling.

7. Thermocouple System

The graphite armor units cover approximately 70% of the circumference of the inner wall and support a total of 60 thermocouples. Each of these four graphite armor units are positioned to intercept injected neutral beams and contain between 14 to 16 thermocouples depending on the local interferences from inner wall diagnostics. These thermocouples are arrayed so as to maximize the information that they can provide on neutral beam position and power density profiles. The Chromel-Alumel thermocouples are held in graphite screws with a ceramic spacer and graphite cement. The graphite screws penetrate the SS-304 backing plate via clearance holes. A threaded hole in the tile allows the thermocouple tip to be securely held 0.64 cm from the tile front face. Figure 10 shows the details of the thermocouple design.

Mounted on the inner wall directly in back of each graphite armor array unit, behind the point of maximum power density, is a 1.27 cm thick 25 xm x 25 cm, SS-304 plate which acts as a final emergency beam stop in the event of a failure of the primary armor. Each of these four final beam stop plates has one thermocouple mounted tightly with a screw 0.68 cm from its front face. Interlock circuits monitor these four thermocouples and are set to interpret any temperature increase above ambient as indicative of a thermal failure in the primary armor and thus inhibit the neutral beam pulse.

The 30% of the inner wall circumference that does not receive direct neutral beam power is armored with titanium plate (see Fig. 1). One of these plates holds a vertical array of 7 thermocouples mounted tightly 0.39 cm from the front face with screws. This plate acts as an inner wall plasma calorimeter for measuring thermal loading during normal operations and disruptions in the plasma current.

The armor is grounded to the PDX vessel which is electrically isolated during shots. The thermocouples are in electrical contact with the armor and, hence, are grounded to the vessel at this point of contact. A thermocouple control circuit disconnects the thermocouples from the external amplifier circuits four seconds before the PDX shot and reconnects them four seconds after the shot. This maintains the electrical isolation of the vessel and prevents the thermocouples and amplifier circuits from providing closed electrical loops to the flow of very high eddy currents. In addition, this control circuit, prior to disconnecting the thermocouples, also scans each thermocouple and measures the resistance across the junction and the resistance between the thermocouple and the vessel. A high resistance is taken as indicative of a cracked or missing tile or a thermocouple malfunction. This inhibits the beam shot until the cause is investigated and an interlock is manually returned to normal.

The thermocouple signals are processed by a CAMAC based DEC PDP11/34 computer system in beam position, and power density p 'es are derived from these signals and displayed for the operators. Anomalous temperatures or thermal distribution patterns are sensed, and the operators are alerted to a possible thermal failure of the armor.

8. Preparation and Installation

Prior to installation, the backing plates were degreased with 500 psi steam, washed in an alkali solution, rinsed with distilled water, and dried by baking at 150°C for 1 hour. The clean units were then tested for vacuum leaks using a standard helium mass spectrometer leak detector. Prior to installation in the backing plates, the TiC/C tiles were baked in a vacuum furnace at 600°C for 8 hours. The tiles were then loaded into the backing plates and the thermocouples were attached. The complete armor subunits with attached tiles, thermocouples, and water manifolds were then placed in the vacuum vessel through an available port.

The procedure inside the vacuum vessel involved accurately positioning the armor support mechanisms on the inner wall opposite each beam line, bolting the subunits on the support arcs, joining the conflat flanges of the water distribution system, and vacuum testing all the water connections for operating internal water pressures of 120 psi and external vacuum pressures of $\sim 2 \times 10^{-8}$ torr.

9. Conclusions

The thermal loads, electromagnetic forces, mechanical vibrations, duty cycle, plasma control requirements, and ultra clean vacuum environment impose many difficult constraints on the design and operation of a wall armor and inner limiter system of the high power PDX Tokamak/Neutral Beam Heating experiment. Many of these constraints will need to be considered in the design of the forthcoming larger fusion devices.

Acknowledgments

The authors wish to acknowledge helpful discussions with K. Bol, H. Eubank, J. Cecchi, F. Dalhgren, F. Dylla, L. Gereg, S. Hand, T. Kozub, D. Meade, K. Owens, G. Schilling, J. Schmidt, L. Stewart, F. Ullrich, A. von Halle, and M. Williams. We also wish to acknowledge the technical contributions of M. Egin, G. Evans, L. Gereg, C. Harrison, C. Loeffler, E. Ryan, R. Shoemaker, and J. Smolinski. Work supported in part by the U.S. Department of Energy, Contract No. DE-AC02-76-CHO-3073.

References

[1] W.L. Gardner et al., "Proceeding of the 8th Symposium on Engineering Problems of Fusion Research," San Francisco, CA 1979, (IEEE, N.Y, N.Y.) p. 972.

[2] M.M. Menon et al., Ibid., p. 656.

[3] J Kim and J.H. Whealton, Nuc. Inst. Meth. 141 (1977) 187.

[4] Provided by L. D. Stewart, Exxon Nuclear Co., Present address, Princeton University, Princeton, N.J. 08540.

[5] J.A. Schmidt, "Comments on Plasma Physics and Controlled Fusion," 5 (1980) 225.

[6] B.M. V. Scherzer, J. Vac. Sci. Technol. 13 (1976) 420.

[7] S.A. Cohen, J. Vac. Sci. Technol. 13 (1976) 449.

[8] J. Craig, Jr., J. Vac. Sci. Technol. 18, (1981) 1046.

[9] POCO Graphite, Inc., Decatur, Texas, 762234.

[10] Ultramet, Inc., Pacoima, California, 91331.

[11] *H.W. Kugel and H.F. Dylla, Princeton University, Princeton, N.J.* (unpublished).

[12] K.L. Wilson, Sandia National Laboratories, Livermore, CA 94550. Private communication 1981.

[13] C. Braganya, G.M. McCracken, and S.K. Erents, "Proceedings of the International Symposium on Plasma Wall Interaction," Jülich, 1976 (Pergammon Press, 1977) 257.

[14] K.L. Wilson and A.E. Pontau, J. Nucl. Mater. 93 & 94 (1980) 569.

[15] M. Ulrickson, "Proceedings of the First Topical Meeting on Fusion Reactor Materials," ed. F.W. Wiffen, J. H. De Van, and J. D. Stiegler (North-Holland Publishing Co., Amsterdam, 1979); J. Nucl. Mater. 85 &

86 (1979) 231. M. Ulrickson and J. Cecchi, Thin Solid Flims 73, 133 (1980). M. Ulrickson, J. Vac. Sci. Technol. 18, (1981) 1037.

[16] H.S. Carslow and J.C. Jaeger, "Conduction of Heat in Solids" (Clarendon Press, Oxford) 1973.

[17] H.F. Dylla, J. Nucl. Mater. 95 (1980) 951.

[18] H.F. Dylla, Princeton University. Private communication.

[19] D.M. Mattox, A.W. Mullendore, H.O. Pierson, and D.J. Sharp, J. Nucl. Mater. 85 & 86, 1127 (1979).

[20] J. Ruth, J. Bohdansky, and A.P. Martinellic, "Int. Conf. on Ion Beam Modification of Materials," Budapest, 1978.

[21] M. Kaminsky, Thin Solid Films 73, 117 (1980).

[22] S.K. Das, M. Kaminsky, and R. Tishler, J. Nucl. Mater. 85 & 86, 225 (1979).

[23] M. Kamisky and R. Nielsen, to be published.

Table 1

Comparison of Some Surface Properties of the Candidate Materials

Material	Z	Y(Rt)[a]	Y(1000°C)[b]	T_m[c]
C	6	0.074[d]	0.10[d]	3500[f]
Ti	22	0.004[e]		1800
TiC	14	0.0094[d]	0.0098[d]	2100-2300[f]
V	23	0.01[g]		1710
Cu	29	0.059[d]		1083

a) Sputtering yield (atoms/ion) for 1 keV protons, for a substrate at room temperature. See also References 21, 22, and 23 for other energies, species, and conditions.

b) Sputtering yield (atoms/ion) for 1 keV protons, for a substrate at 1000° C.

c) Melting temperature in degrees C.

d) Ref. 19.

e) Ref. 20.

f) Sublimation temperature.

g) Reference 21 D^+ yield and Ref. 19 $y = 5.0 \times 10^{-4}$ for 0.25 keV H^+.

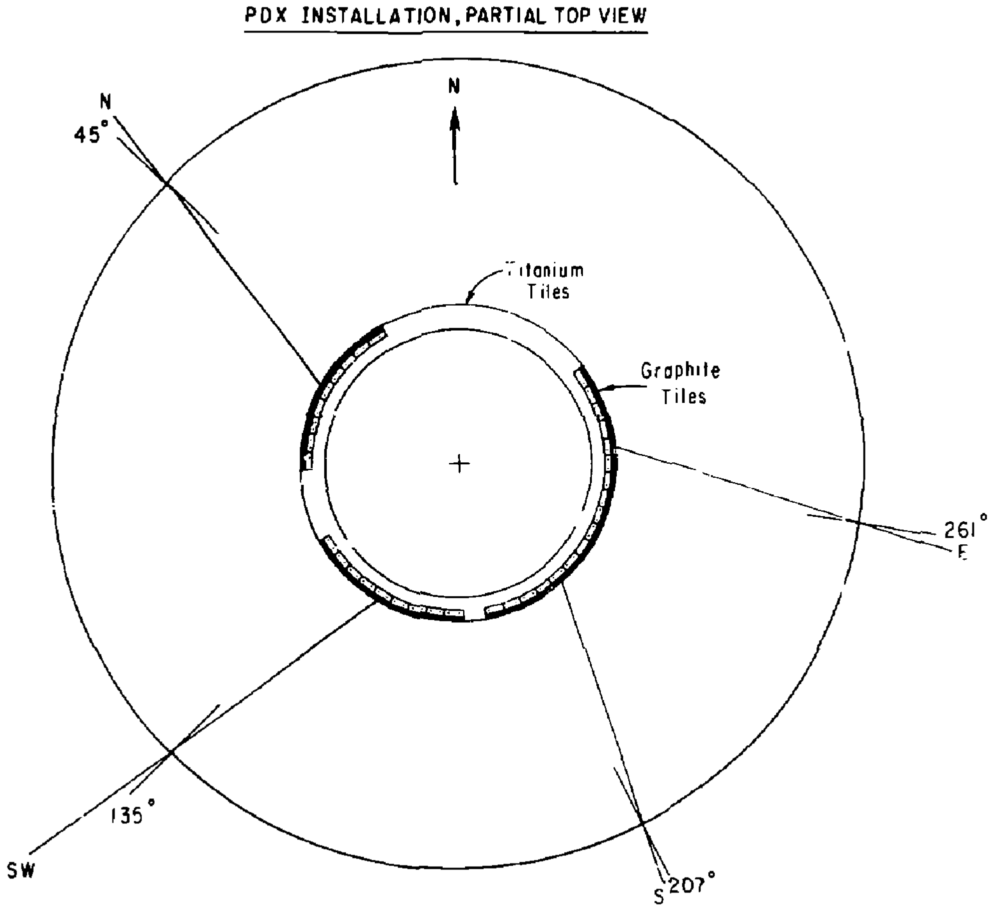

Fig. 1 A partial schematic top view showing the location and injection angles of the PDX neutral beam injection system. Shown also are the locations of the coated graphite and titanium inner wall armor.

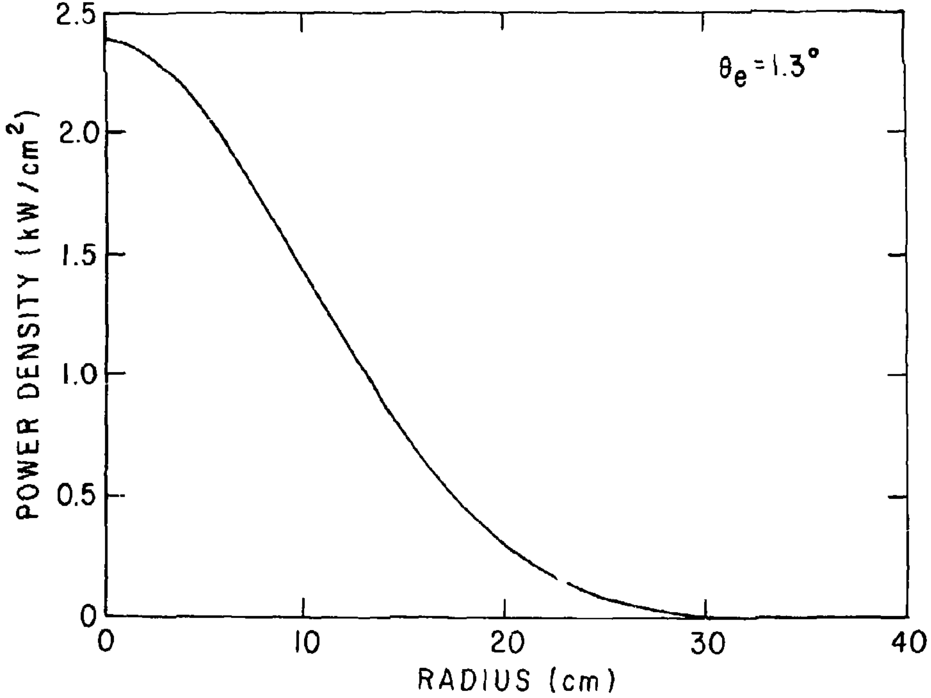

Fig. 2 A calculated typical power density profile at the inner wall of PDX.

81X0262

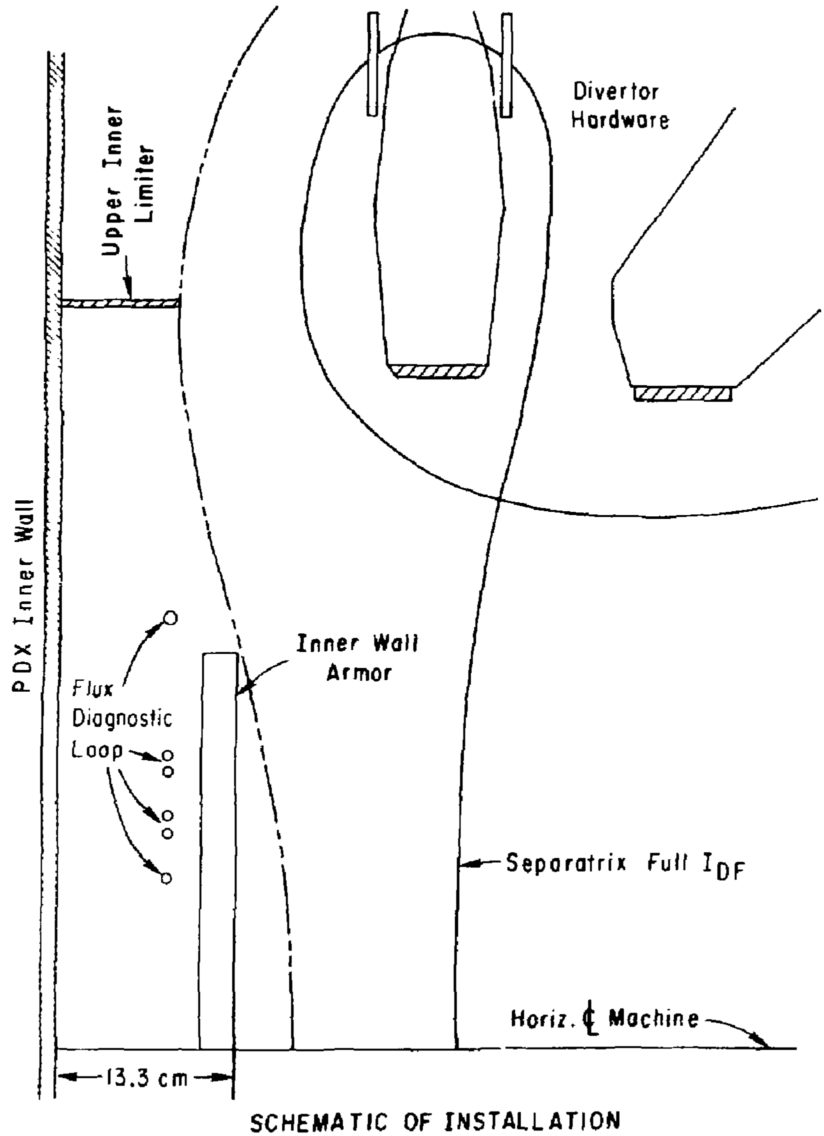

Fig. 3 A partial schematic diagram showing a cross-section view of the inner wall region of PDX.

61 X 0258

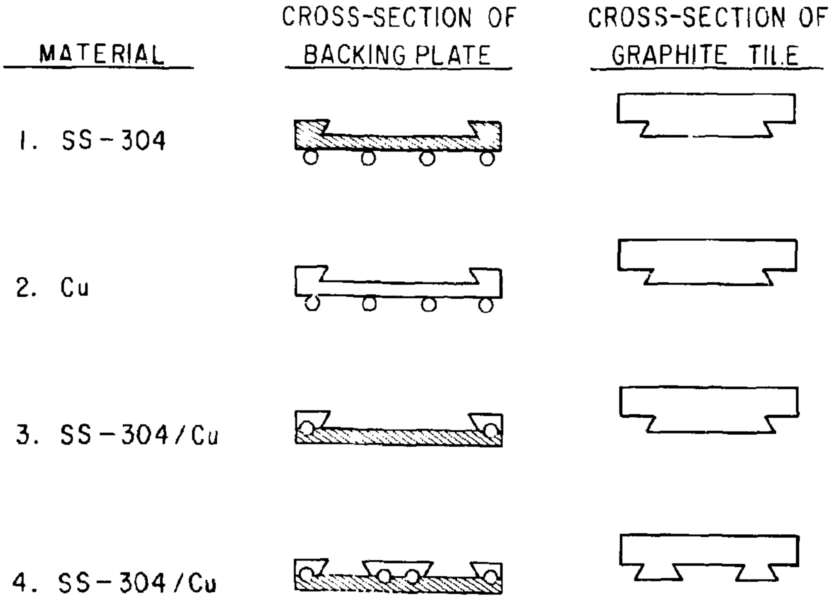

Fig. 4 Summary of the materials and designs tested for the TiC/C tile backing plates.

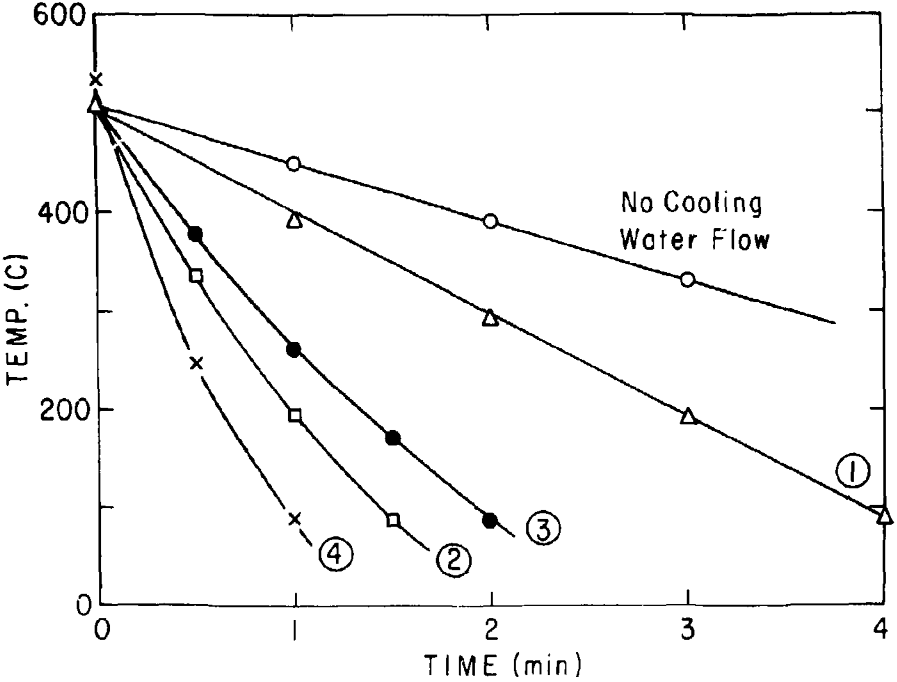

Fig. 5 Measured front face temperature versus time of POCO graphite tiles supported by various types of water cooled backing plates. The test units were heated to a uniform front face initial temperature of 500°C. The circled numbers refer to the design types shown in Fig. 4. Refer to text.

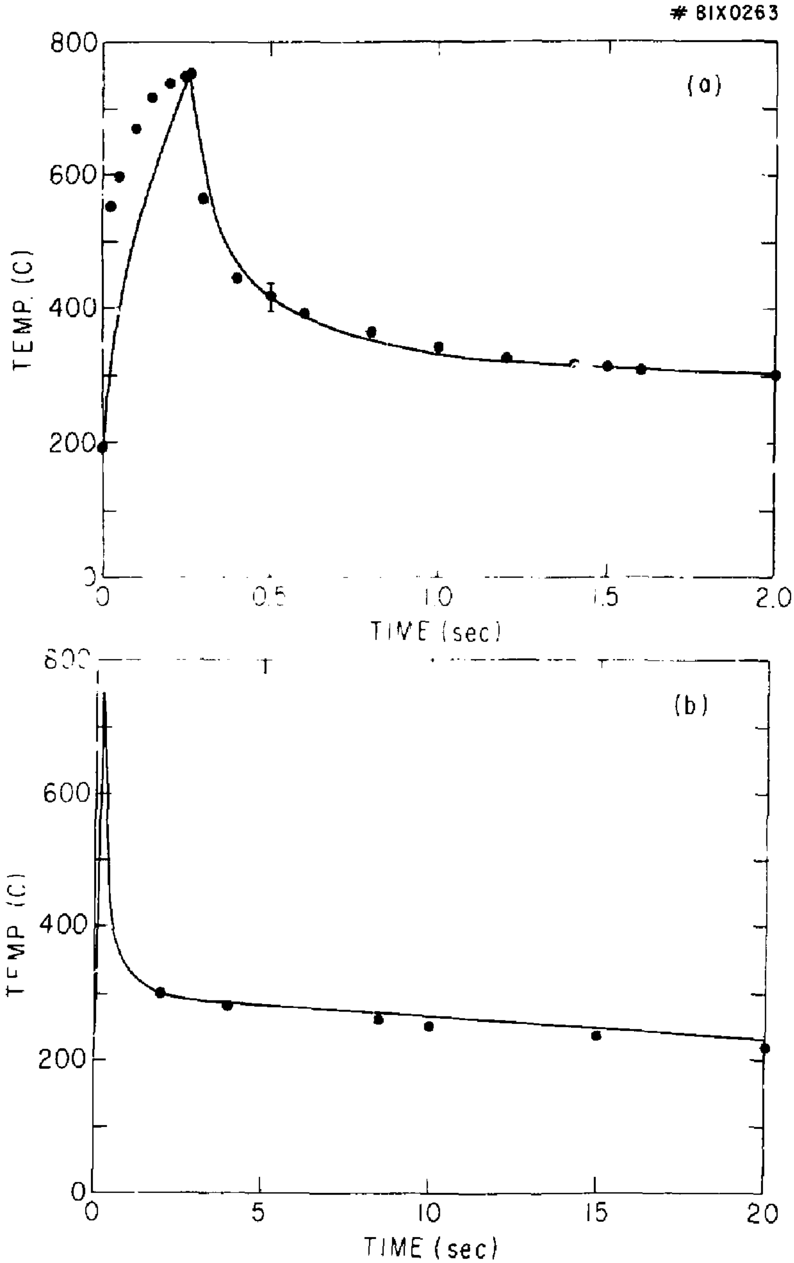

Fig. 6 Measurements of the front face temperature versus time of the prototype tile and backing plate design. a) 0 to 2 secs, and b) 0 to 20 secs. The tile was heated by a 40 kV, 2.5 kW/cm^2, 250 msec H^0 pulse. The solid line is the result of a theoretical calculation.

#81X0260

GRAPHITE-SLAT ALIGNMENT

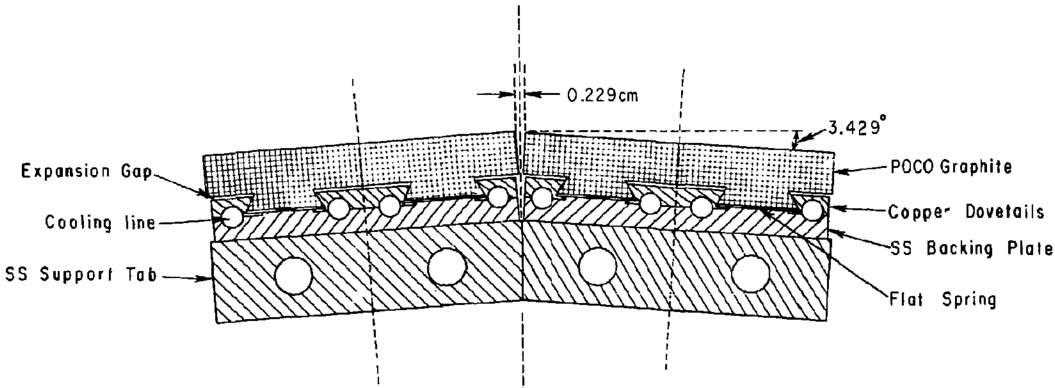

Partial Top View
(Full Scale)

Fig. 7 Partial schematic cross-section end view of the final graphite tile and backing plate alignment.

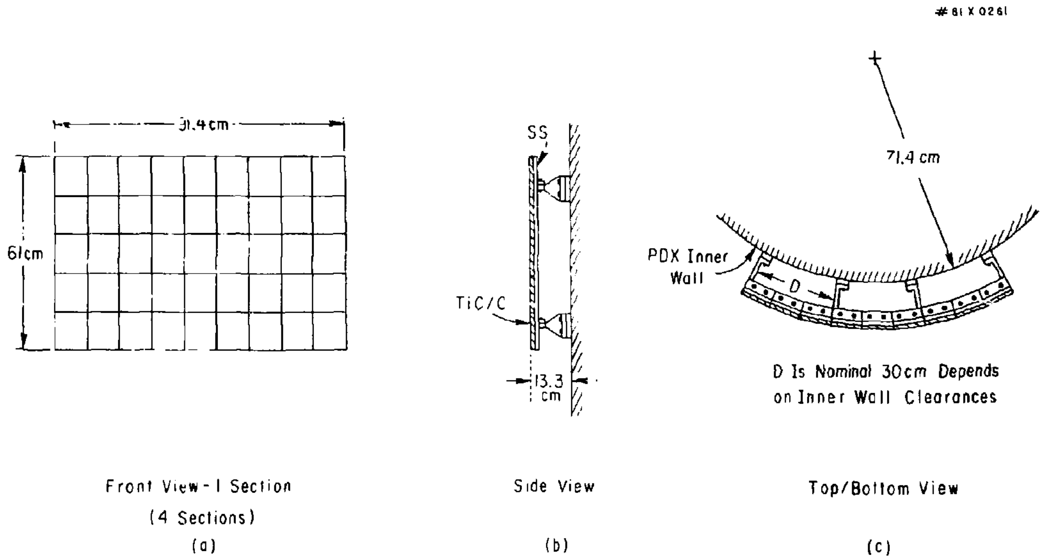

Fig. 8 Partial schematic diagrams showing details of the PDX neutral beam armor and supports.

#81X 0257

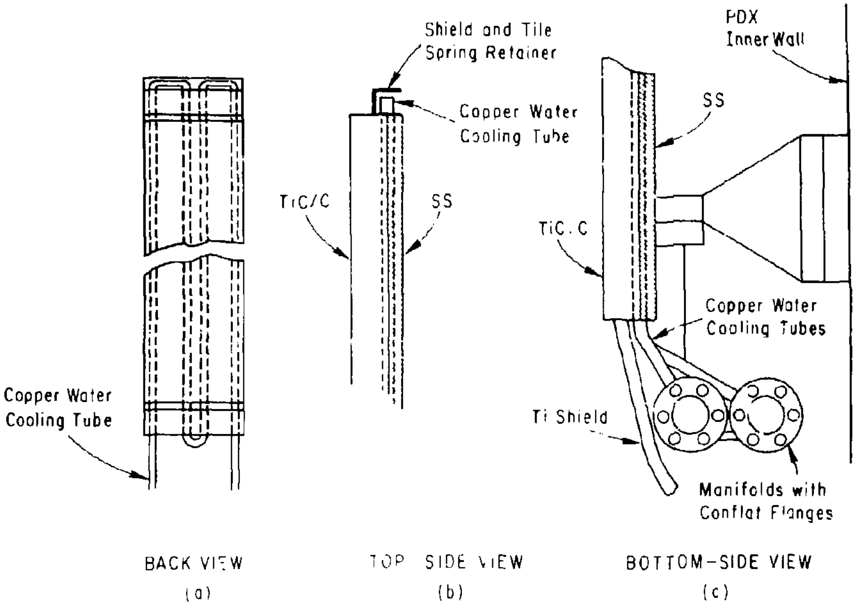
Shield and Tile
Spring Retainer
Copper Water
Cooling Tube
TiC/C
SS
PDX
Inner Wall
SS
TiC.C
Copper Water
Cooling Tubes
Copper Water
Cooling Tube
Ti Shield
Manifolds with
Conflat Flanges
BACK VIEW
(a)
TOP SIDE VIEW
(b)
BOTTOM-SIDE VIEW
(c)

81X0256

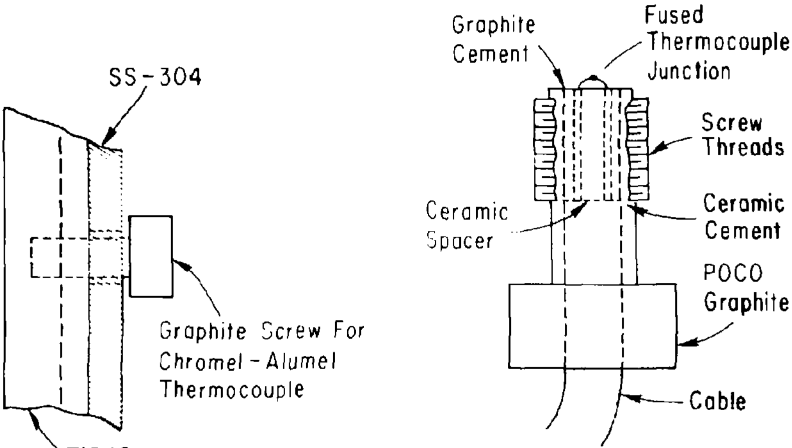

(a) (b)

Fig. 10 A partial schematic diagram of the thermocouple design for the graphite tiles.